Quantum Fisher information of entangled coherent states in the presence of photon loss

Y. M. Zhang,[1] X. W. Li,[1] W. Yang,[2,*] and G. R. Jin[1,†]
[1]*Department of Physics, Beijing Jiaotong University, Beijing 100044, China*
[2]*Beijing Computational Science Research Center, Beijing 100084, China*
(Received 28 July 2013; published 17 October 2013)

We investigate the performance of entangled coherent states for quantum-enhanced phase estimation. An exact analytical expression of quantum Fisher information is derived to show the role of photon losses on the ultimate phase sensitivity. We find a transition of the sensitivity from the Heisenberg scaling to the classical scaling due to quantum decoherence of the photon state. This quantum-classical transition is uniquely determined by the number of photons being lost, instead of the number of incident photons or the photon loss rate alone. Our results also reveal that a crossover of the sensitivity between the entangled coherent state and the NOON state can occur even for very small photon loss rate.

DOI: 10.1103/PhysRevA.88.043832 PACS number(s): 42.50.St, 42.50.Lc, 03.65.Ta, 06.20.Dk

I. INTRODUCTION

The estimation of parameters characterizing dynamical processes is essential to science and technology. A typical parameter estimation consists of three steps. First, the input state $|\psi_{\rm in}\rangle$ of the sensor is prepared. Second, the sensor undergoes the ϕ-dependent dynamical process $\hat{U}(\phi)$ and evolves to the output state $|\psi\rangle$. Finally, a measurement is made on the output state, and the outcome x is used by suitable data processing to produce an unbiased estimator $\hat{\phi}(x)$ of the parameter ϕ. The precision of the estimation is quantified by the standard deviation $\delta\phi = \langle[\hat{\phi}(x)-\phi]^2\rangle$, which is determined by the input state $|\psi_{\rm in}\rangle$ [1–7], the nature of the dynamical process $\hat{U}(\phi)$ [8–13], the observable being measured [14–18], and the specific data-processing technique. The precision of the estimator $\hat{\phi}_{\rm opt}(x)$ from optimal data processing is limited by the Cramér-Rao inequality [19,20] as $\delta\phi_{\rm opt} \geqslant 1/\sqrt{F(\phi)}$, where $F(\phi)$ is the classical Fisher information, determined by $|\psi_{\rm in}\rangle$, $\hat{U}(\phi)$, and the measurement scheme. Given $|\psi_{\rm in}\rangle$ and $\hat{U}(\phi)$, maximizing $F(\phi)$ over all possible measurements gives the quantum Fisher information (QFI) F_Q and hence the quantum Cramér-Rao bound $\delta\phi_{\rm min} = 1/\sqrt{F_Q}$ [21–25] on the attainable precision to estimate the phase ϕ.

In general, the best precision $\delta\phi_{\rm min}$ improves with an increasing number of resources N employed in the measurement, e.g., the number of photons in optical phase estimation or the total duration of measurements in high-precision magnetic-field or electric-field sensing. For separable input states, the QFI $F_Q \sim N$ gives the classical limit $\delta\phi_{\rm min} \sim 1/\sqrt{N}$, in agreement with the classical central limit theorem. To obtain an enhanced precision, it is necessary to utilize quantum resources such as coherence, entanglement, and squeezing in the input state for maximizing the QFI and hence the precision. This is a central issue in quantum metrology [26–31]. In the absence of noise, it has been well established that by utilizing quantum entanglement, the QFI can be enhanced up to $F_Q \sim N^2$ and hence the precision $\delta\phi_{\rm min} \sim 1/N$, reaching the Heisenberg limit [4–7,32–35]. This limit is the ultimate estimation precision allowed by a quantum resource with a definite particle number. In the presence of noise, however, it is not clear whether the Heisenberg limit can still be achieved [36–38] and whether entanglement is still a useful resource for quantum metrology.

A paradigmatic example is the estimation of the relative phase shift between the two modes propagating on different arms of the Mach-Zehnder interferometer (MZI). Precise phase estimation is important for multiple areas of scientific research [17], such as imaging, sensing, and information processing. In the absence of noise, the classical limit $\delta\phi_{\rm min} \sim 1/\sqrt{\bar{n}}$ ($\bar{n}$ is the average number of photons) for a classical coherent state can be dramatically improved by using nonclassical states of the light. The maximally entangled NOON states $\sim|N,0\rangle_{1,2} + |0,N\rangle_{1,2}$ [also called the Greenberger-Horne-Zeilinger (GHZ) state in atomic spectroscopy] have been prepared in experiments for pursuing the Heisenberg-limited phase estimation [4–6]. However, the NOON states are extremely sensitive to photon losses [36–45]. In a lossy interferometer, it has been shown that a transition of the precision from the Heisenberg limit to the shot-noise limit can occur with the increase of particle number N [37,38].

Recently, a specific coherent superposition of the NOON states, the entangled coherent state (ECS) $\sim|\alpha,0\rangle_{1,2} + |0,\alpha\rangle_{1,2}$, was proposed as the input state for enhanced precision [43]. In the absence of photon losses, the precision of the ECS can surpass that of the NOON state (i.e., the Heisenberg limit, $\delta\phi_{\rm min} = 1/\bar{n}$). In the presence of photon losses, numerical simulation suggests that the ECS outperforms the NOON state for photon numbers $\bar{n} \lesssim 5$. For a small photon number $\bar{n} \sim 5$, the precision is better than the classical limit by a factor $\sqrt{\bar{n}} \sim 2$. To achieve more significant enhancement for practical applications, much larger photon numbers are required. The performance with a large number of resources is an important benchmark for a realistic quantum-enhanced estimation scheme. Therefore, a careful analysis of the QFI and the ultimate precision for the input ECS with large $\bar{n}$ is necessary.

In this paper, we present an exact analytical result of the QFI for the entangled coherent state with arbitrary $\bar{n}$, which provides counterintuitive physics that is inaccessible from previous numerical simulations. To understand why the ECS is better than the NOON state, we first consider an arbitrary superposition of the NOON states and find the QFI $F_Q \geqslant \bar{n}^2$,

*wenyang@csrc.ac.cn
†grjin@bjtu.edu.cn

leading to a sub-Heisenberg-limited sensitivity $\delta\phi_{\min} \leqslant 1/\bar{n}$. Next, we investigate the role of photon losses on the QFI and hence the ultimate precision of the ECS. An exact result of the QFI is derived, which is the sum of the classical term $\propto\bar{n}$ and the Heisenberg term $\propto\bar{n}^2$. We show that the photon losses suppress exponentially the off-diagonal (coherence) part of the reduced density matrix $\hat{\rho}$ and hence the Heisenberg term, while leaving the classical term largely unchanged. The loss-induced quantum decoherence leads to a transition of the estimation precision from the Heisenberg scaling to the classical scaling as the number of lost photons $R\bar{n}$ increases, where R is the photon loss rate and $\bar{n}$ is the mean photon number of the initial ECS. This behavior is in sharp contrast to the NOON state, for which the photon losses eliminate completely the phase information stored in the coherence part of $\hat{\rho}$. The ultimate precision of the NOON state gets even worse than the classical limit when $R\bar{n} \gg 1$. Surprisingly, we find that the precision of the NOON state may be better than that of the ECS within the crossover region at $R\bar{n} \sim 1$. This is because although the classical term of the ECS is robust against the photon losses, the Heisenberg term decays about twice as quickly as that of the NOON state.

II. SUB-HEISENBERG-LIMITED PHASE SENSITIVITY WITH A SUPERPOSITION OF NOON STATES

First, let us consider an *arbitrary* coherent superposition of the NOON states as the input state after the first beam splitter of a two-mode MZI,

$$|\psi_{\rm in}\rangle = \sum_{n=0}^{\infty} c_n \frac{|n\rangle_1 + |n\rangle_2}{\sqrt{2}}, \tag{1}$$

where, for brevity, we introduce the notation $|n\rangle_1 \equiv |n\rangle_1|0\rangle_2$ and $|n\rangle_2 \equiv |0\rangle_1|n\rangle_2$, representing n photons in mode 1 (or 2) and the other mode in vacuum. To analyze possible achievable phase sensitivity with $|\psi_{\rm in}\rangle$, we directly evaluate the QFI of the outcome state after phase accumulation $|\psi(\phi)\rangle = \hat{U}(\phi)|\psi_{\rm in}\rangle = e^{i\phi\hat{G}}|\psi_{\rm in}\rangle$, where $\hat{G}$ is the generator of phase shift. For a lossless MZI, $|\psi\rangle$ is a pure state, and the QFI is given by the well-known formula [21–25] $F_Q = 4(\langle\psi'|\psi'\rangle - |\langle\psi'|\psi\rangle|^2) = 4(\langle\hat{G}^2\rangle - \langle\hat{G}\rangle^2)$, where $|\psi'\rangle \equiv \partial|\psi\rangle/\partial\phi$ and the expectation values are taken with respect to $|\psi_{\rm in}\rangle$. Considering a linear phase-shift generator $\hat{G} = \hat{n}_2$ [36,43], with the photon number operators $\hat{n}_2 = \hat{a}_2^\dagger\hat{a}_2$ and $\hat{n}_1 = \hat{a}_1^\dagger\hat{a}_1$, we obtain the QFI

$$F_Q = 4(\langle\hat{n}_2^2\rangle - \langle\hat{n}_2\rangle^2) = 2\langle\hat{n}^2\rangle - \langle\hat{n}\rangle^2, \tag{2}$$

where we have used the relation $\langle\hat{n}_1^l\rangle = \langle\hat{n}_2^l\rangle = \langle\hat{n}^l\rangle/2$ (for $l = 1,2,\ldots$), which, together with $\langle\hat{n}_1\hat{n}_2\rangle = 0$, is valid for Eq. (1). Since $\langle\hat{n}^2\rangle \geqslant \langle\hat{n}\rangle^2$, we have $F_Q \geqslant \bar{n}^2$, where $\bar{n} = \langle\hat{n}\rangle$ is the mean photon number of $|\psi_{\rm in}\rangle$. This inequality also applies to another kind of phase-shift generator $\hat{G} = (\hat{n}_2 - \hat{n}_1)/2$, for which $F_Q = \langle\hat{n}^2\rangle$. They suggest that a sub-Heisenberg-limited phase sensitivity $\delta\phi_{\min} < 1/\bar{n}$ can be achieved with an arbitrary coherent superposition of the NOON states, likes Eq. (1). The equality $\delta\phi_{\min} = 1/\bar{n}$, known as the Heisenberg limit, is attainable for the NOON state [4–7,32–35]: $(|N\rangle_1 + |N\rangle_2)/\sqrt{2}$ with $\bar{n} = N$.

Next, we review the recently proposed ECS state [46,47]: $\mathcal{N}_\alpha(|\alpha\rangle_1 + |\alpha\rangle_2)$ as a special case of the superposition of NOON states, where $\mathcal{N}_\alpha = [2(1 + e^{-|\alpha|^2})]^{-1/2}$ is the normalization constant and $|\alpha\rangle_1 \equiv |\alpha\rangle_1|0\rangle_2$ denotes a coherent state in sensor mode 1 and vacuum in sensor mode 2 and similarly for $|\alpha\rangle_2 \equiv |\alpha\rangle_2|0\rangle_1$. The input ECS is now experimentally feasible for the coherent amplitude $\alpha \sim 1.5$ [43,48]. In addition, using the ECS as the input state and considering the phase accumulation dynamics $\hat{U}(\phi) = e^{i\phi\hat{n}_2}$ [36,43], we obtain $\bar{n} = \langle\hat{n}\rangle = 2\mathcal{N}_\alpha^2|\alpha|^2$, $\langle\hat{n}^2\rangle = 2\mathcal{N}_\alpha^2|\alpha|^2(|\alpha|^2 + 1)$, and hence the quantum Fisher information

$$F_Q = 2\bar{n}[1 + w(\bar{n}e^{-\bar{n}})] + \bar{n}^2, \tag{3}$$

where we have used $\bar{n} = |\alpha|^2/(1 + e^{-|\alpha|^2})$ and thereby $|\alpha|^2 = \bar{n} + w(\bar{n}e^{-\bar{n}})$. Here, $w(z)$ denotes the Lambert W function (also called the product logarithm), which gives the principal solution for w in $z = we^w$. For mean photon number $\bar{n} \approx |\alpha|^2 \gg 1$, we have $w(\bar{n}e^{-\bar{n}}) \approx 0$ and $F_Q \approx \bar{n}(\bar{n} + 2)$. From Fig. 1(a), one can find that $\delta\phi_{\min}$ of the ECS [the blue (dark gray) solid line] is better than that of the NOON [the blue (dark gray) dashed line], especially for a modest photon number. A recent numerical simulation shows that this improved sensitivity of the ECS can be maintained in the presence of the photon losses for $\bar{n} \lesssim 5$ [43]. However, the performance of the ECS with larger $\bar{n}$ remains unclear.

III. QUANTUM FISHER INFORMATION AND ULTIMATE PRECISION OF THE ENTANGLED COHERENT STATE WITH PHOTON LOSSES

In this section, we present an exact analytical expression of the QFI F_Q and hence the ultimate precision $\delta\phi_{\min} = 1/\sqrt{F_Q}$ for the ECS in the presence of photon losses. This provides detailed information for the performance of the ECS in the quantum phase estimation, especially those states at relatively large photon numbers, that is inaccessible from the previous numerical simulation. First, we derive an exact analytical expression of the quantum Fisher information for the input ECS based upon a general formula of the QFI. This formula decomposes the total QFI into three physically intuitive contributions. Next, we present the QFI of the NOON state. Finally, by comparing with the NOON state, we discuss the key features of the ECS and provide a simple physics picture.

The photon losses can be modeled by inserting two identical beam splitters $\hat{B}_{k,k'}(\theta) = \exp[i(\theta/2)(\hat{a}_{k'}^\dagger\hat{a}_k + \text{H.c.})]$ that couple two sensor modes $k = 1, 2$ and two environment modes $k' = 1', 2'$ that are initially in the vacuum [36–45]. The action of the beam splitters transforms the sensor mode $\hat{a}_k^\dagger$ into a linear combination of $\hat{a}_k^\dagger$ and $\hat{a}_{k'}^\dagger$: $\hat{B}_{k,k'}\hat{a}_k^\dagger\hat{B}_{k,k'}^{-1} = \sqrt{T}\hat{a}_k^\dagger + i\sqrt{R}\hat{a}_{k'}^\dagger$, where $T = \cos^2(\theta/2)$ and $R = 1 - T$ are transmission and absorption (loss) rates of the photons, respectively. More specifically, $T = 1$ (i.e., $R = 0$) means no photon loss, and $T = 0$ ($R = 1$) corresponds to complete photon loss. For the input ECS state, using $\hat{U}(\phi)|\alpha\rangle_2 = |\alpha e^{i\phi}\rangle_2$ and $\hat{B}_{k,k'}|\alpha\rangle_k = |\sqrt{T}\alpha\rangle_k|i\sqrt{R}\alpha\rangle_{k'}$, we obtain the outcome state

$$\begin{aligned}|\psi(\phi)\rangle &= \mathcal{N}_\alpha\hat{B}_{1,1'}\hat{B}_{2,2'}\hat{U}(\phi)(|\alpha\rangle_1 + |\alpha\rangle_2)|0\rangle_{1'}|0\rangle_{2'}\\ &= \mathcal{N}_\alpha(|\sqrt{T}\alpha\rangle_1|E^{(1)}\rangle + |\sqrt{T}\alpha e^{i\phi}\rangle_2|E^{(2)}\rangle),\end{aligned}$$

where the environment states are given by $|E^{(1)}\rangle \equiv |i\sqrt{R}\alpha\rangle_{1'}|0\rangle_{2'}$ and $|E^{(2)}\rangle \equiv |0\rangle_{1'}|i\sqrt{R}\alpha e^{i\phi}\rangle_{2'}$. Tracing over

them, we obtain the reduced density matrix of the sensor modes

$$\hat{\rho} = \mathcal{N}_\alpha^2\{|\sqrt{T}\alpha\rangle_{11}\langle\sqrt{T}\alpha| + |\sqrt{T}\alpha e^{i\phi}\rangle_{22}\langle\sqrt{T}\alpha e^{i\phi}| + \langle E^{(2)}|E^{(1)}\rangle(|\sqrt{T}\alpha\rangle_{12}\langle\sqrt{T}\alpha e^{i\phi}| + \text{H.c.})\}, \quad (4)$$

where $\langle E^{(2)}|E^{(1)}\rangle = \langle E^{(1)}|E^{(2)}\rangle = e^{-R|\alpha|^2}$. Compared with the lossless case (i.e., $T = 1$), the amplitudes in the sensor modes are reduced from $|\alpha|$ to $\sqrt{T}|\alpha|$. More importantly, the photon losses suppress the off-diagonal coherence between the two sensor states by a factor of $\langle E^{(2)}|E^{(1)}\rangle$. We will show below that this decoherence effect significantly degrades the estimation precision of the ECS.

Since $\hat{\rho}$ is a mixed state, to obtain the QFI one has to diagonalize it as $\hat{\rho} = \sum_m \lambda_m|\lambda_m\rangle\langle\lambda_m|$, where $\{|\lambda_m\rangle\}$ forms an orthonormalized and complete basis, with λ_m being the weight of $|\lambda_m\rangle$. According to the well-known formula [21,22,26,27], the QFI is given by

$$F_Q = \sum_{m,n} \frac{2}{\lambda_m + \lambda_n}|\langle\lambda_m|\hat{\rho}'|\lambda_n\rangle|^2, \quad (5)$$

where the prime denotes the derivation about ϕ, such as $\hat{\rho}' = \partial\hat{\rho}/\partial\phi$, $\lambda_m' = \partial\lambda_m/\partial\phi$, and $|\lambda_m'\rangle = \partial|\lambda_m\rangle/\partial\phi$. Typically, the dimension of the entire Hilbert space and hence the basis $\{|\lambda_m\rangle\}$ is huge, but only a small subset has nonzero weights. Therefore, using the completeness and the orthonormalization of $\{|\lambda_m\rangle\}$, we can express the QFI in terms of the subset $\{|\lambda_i\rangle\}$ with $\lambda_i \neq 0$ (see Appendix):

$$F_Q = \sum_i \frac{(\lambda_i')^2}{\lambda_i} + \sum_i \lambda_i F_{Q,i} - \sum_{i\neq j} \frac{8\lambda_i\lambda_j}{\lambda_i + \lambda_j}|\langle\lambda_i'|\lambda_j\rangle|^2, \quad (6)$$

which contains three kinds of contributions. The first term is the classical Fisher information for the probability distribution $P(i|\phi) \equiv \lambda_i(\phi)$. The second term is a weighted average over the quantum Fisher information $F_{Q,i} = 4(\langle\lambda_i'|\lambda_i'\rangle - |\langle\lambda_i'|\lambda_i\rangle|^2)$ for each pure state in the subset $\{|\lambda_i(\phi)\rangle\}$, with $\lambda_i \neq 0$. The last term reduces the QFI and hence the estimation precision below the pure-state case. If the phase shift ϕ comes into the reduced density matrix $\hat{\rho}$ through the weights $\lambda_i(\phi)$ only, then the last two terms of Eq. (6) give a vanishing contribution to the QFI. For ϕ-independent weights, however, the first term vanishes, in agreement with the previous result [42].

Compared with Eq. (5), which relies on the complete basis, our formula (6), defined within a truncated Hilbert space, has the advantages of faster convergence and numerical stability, especially when the reduced density matrix $\hat{\rho}$ has some eigenvectors with extremely small but nonvanishing weights.

For the input ECS, we note that the reduced density matrix $\hat{\rho}$ only contains two sensor states, $|\sqrt{T}\alpha\rangle_1$ and $|\sqrt{T}\alpha e^{i\phi}\rangle_2$ [see Eq. (4)]. This feature enables us to expand $\hat{\rho}$ in terms of two eigenvectors with nonzero eigenvalues (see Appendix A),

$$\hat{\rho} = \lambda_+ |\lambda_+(\phi)\rangle\langle\lambda_+(\phi)| + \lambda_- |\lambda_-(\phi)\rangle\langle\lambda_-(\phi)|, \quad (7)$$

where the eigenvalues $\lambda_\pm = \mathcal{N}_\alpha^2(1 \pm e^{-R|\alpha|^2})(1 \pm e^{-T|\alpha|^2})$ are ϕ independent and obey $\lambda_- + \lambda_+ = 1$. The phase-dependent eigenvectors are given by

$$|\lambda_\pm(\phi)\rangle = \eta_\pm[\pm|\sqrt{T}\alpha\rangle_1 + |\sqrt{T}\alpha e^{i\phi}\rangle_2], \quad (8)$$

with the normalization factors $\eta_\pm = 1/\sqrt{2(1 \pm e^{-T|\alpha|^2})}$. It is easy to prove that $\langle\lambda_\pm|\lambda_\pm\rangle = 1$ and $\langle\lambda_+|\lambda_-\rangle = \langle\lambda_+|\hat{\rho}|\lambda_-\rangle = 0$.

Using Eq. (6), we obtain an exact analytical expression of the QFI (see Appendix B):

$$F_Q = F_Q^{\text{cl}} + F_Q^{\text{HL}}, \quad (9)$$

where the classical term $F_Q^{\text{cl}} = 2\bar{n}T[1 + Tw(\bar{n}e^{-\bar{n}})]$ and the Heisenberg term

$$F_Q^{\text{HL}} = (\bar{n}T)^2\left(\frac{e^{-2R|\alpha|^2} - e^{-2T|\alpha|^2}}{1 - e^{-2T|\alpha|^2}}\right). \quad (10)$$

In the absence of photon losses (i.e., $R = 0$ and $T = 1$), our result reduces to the lossless case, i.e., Eq. (3). Compared with it, we find that the photon losses lead to two effects on the QFI (and hence the estimation precision). First, it trivially reduces the photon number from $\bar{n}$ in the input state to $\bar{n}T$ in the output state. Second, it exponentially suppresses the QFI from $F_Q^{\text{HL}} \sim (\bar{n}T)^2$ to the classical scaling $\sim 2\bar{n}T$ (see below).

For a comparison, we also employ Eq. (6) to derive the QFI for the NOON state $(|N\rangle_1 + |N\rangle_2)/\sqrt{2}$. It is easy to write down the reduced density matrix in a diagonal form:

$$\hat{\rho} = \sum_{n=0}^{N-1} \lambda_n(|n\rangle_{11}\langle n| + |n\rangle_{22}\langle n|) + T^N|\psi_{\text{NOON}}\rangle\langle\psi_{\text{NOON}}|, \quad (11)$$

where the first part is an incoherent mixture of Fock states $|n\rangle_1$ and $|n\rangle_2$ with ϕ-independent weights $\lambda_n = \binom{N}{n}T^n R^{N-n}/2$. The phase information is stored in the second part, $|\psi_{\text{NOON}}\rangle = (|N\rangle_1 + e^{iN\phi}|N\rangle_2)/\sqrt{2}$, which, for the lossless case, gives the QFI N^2. Therefore, according to Eq. (6), the total QFI is equal to the QFI of $|\psi_{\text{NOON}}\rangle$ times its weight T^N, namely,

$$F_{Q,\text{NOON}} = N^2T^N, \quad (12)$$

in agreement with Ref. [36]. With increasing photon number N, the ultimate precision $\delta\phi_{\min} = T^{-N/2}/N$ shows a global minimum at $N_{\text{opt}} = -2/\ln T \approx 2/R$ (as $T = 1 - R \approx e^{-R}$ for small R), indicated by the arrows in Fig. 1(a).

In Fig. 1(a), we plot $\delta\phi_{\min}$ of the ECS (the NOON) state as a function of the number of photons $\bar{n}$ (N) for the transmission rates $T = 0.8$, 0.9, and 1 (from top to bottom). Regardless of T, one can find that $\delta\phi_{\min}$ of the input ECS decreases monotonically with the increase of $\bar{n}$. For the NOON state, however, $\delta\phi_{\min}$ reaches its minimum at N_{opt} and then grows rapidly. In Fig. 1(b), we show $\delta\phi_{\min}$ against T for $\bar{n}$ (N) = 4 and 20. It is interesting to note that a crossover of $\delta\phi_{\min}$ between the ECS and the NOON states occurs for large $\bar{n}$ and T (say, $T > 0.85$).

We now analyze the QFI under practical conditions: $T \sim 1$ ($R \sim 0$) and $|\alpha|^2 \gg 1$, for which $w(\bar{n}e^{-\bar{n}}) \approx 0$ and hence $|\alpha|^2 \approx \bar{n}$. In addition, the exponential term $e^{-2T|\alpha|^2}$ of Eq. (10) is negligible. As a result, the QFI reduces to

$$F_Q = F_Q^{\text{cl}} + F_Q^{\text{HL}} \approx 2\bar{n}T + (\bar{n}T)^2e^{-2R\bar{n}}, \quad (13)$$

where the exponential term $e^{-2R\bar{n}} = |\langle E^{(2)}|E^{(1)}\rangle|^2$ quantifies the off-diagonal coherence between the two sensor states [see Eq. (4)]. When the number of photons being lost $R\bar{n} = (1 - T)\bar{n} \ll 1$, the Heisenberg term $F_Q^{\text{HL}} \approx (\bar{n}T)^2e^{-2R\bar{n}}$ dominates, and the ultimate precision obeys $\delta\phi_{\min}^{\text{HL}} \approx e^{R\bar{n}}/(\bar{n}T)$. With the increase of $R\bar{n}$, the classical term $F_Q^{\text{cl}} \approx 2\bar{n}T$ becomes important. As $R\bar{n} \gg 1$, a complete decoherence of the two

sensor states occurs due to $|\langle E^{(2)}|E^{(1)}\rangle|^2 \to 0$, leading to the completely mixed state

$$\hat{\rho} \approx \frac{1}{2}(|\sqrt{T}\alpha\rangle_{11}\langle\sqrt{T}\alpha| + |\sqrt{T}\alpha e^{i\phi}\rangle_{22}\langle\sqrt{T}\alpha e^{i\phi}|), \quad (14)$$

where the first term $|\sqrt{T}\alpha\rangle_{11}\langle\sqrt{T}\alpha|$ carries no phase information and hence $F_{Q,1} = 0$ and the ϕ-dependent second term $|\sqrt{T}\alpha e^{i\phi}\rangle_{22}\langle\sqrt{T}\alpha e^{i\phi}|$ produces the pure-state QFI $F_{Q,2} \approx 4\bar{n}T$. Therefore, according to Eq. (6), the total QFI of $\hat{\rho}$ reads $F_Q \approx \sum_i \lambda_i F_{Q,i} \approx 2\bar{n}T$, which in turn gives the classical scaling of the sensitivity $\delta\phi_{\min} \approx \delta\phi_{\min}^{\rm cl} \approx 1/\sqrt{2\bar{n}T}$. In Fig. 2, we present the log-log plot of $\delta\phi_{\min}$ for the loss rate $R = 0.1$ and 0.01. As shown by the red solid lines, the simple formula of Eq. (13) agrees quite well with the exact result (the solid circles). They both show a turning point at $\bar{n} \sim 1/R$. Indeed, the quantum-classical crossover takes place when the Heisenberg term $F_Q^{\rm HL}$ is comparable to the classical term $F_Q^{\rm cl}$, i.e., $R\bar{n} \sim 1$.

For the ECS with large photon losses, i.e., $R\bar{n} \gg 1$, the ultimate precision $\delta\phi_{\min}$ obeys the classical scaling $1/\sqrt{2\bar{n}T}$, which is confirmed by Fig. 2. The precision of the NOON state is optimal at $\bar{n} = -2/\ln T \approx 2/R$ and then rapidly degrades below the classical limit [see the dashed lines, and also Fig. 1(a)]. This is in sharp contrast to the ECS state. Qualitatively, different behaviors of the two states arise from the different influences of photon losses.

(1) For the ECS $\sim|\alpha\rangle_1 + |\alpha\rangle_2$, the off-diagonal coherence between the two sensor states $|\sqrt{T}\alpha\rangle_1$ and $|\sqrt{T}\alpha e^{i\phi}\rangle_2$ is exponentially suppressed by the photon losses, but the diagonal components of $\hat{\rho}$ still carry the phase information [see Eq. (14)], which contributes the QFI $F_Q \approx 2\bar{n}T$.

(2) For the NOON state $\sim|N\rangle_1 + |N\rangle_2$, the phase information is stored only in the coherence part of $\hat{\rho}$ [see Eq. (11)], which decays with the photon losses as $T^N \approx e^{-RN}$ for small R. When the lost photon number $RN \gg 1$, the information about the phase shift ϕ is completely eliminated.

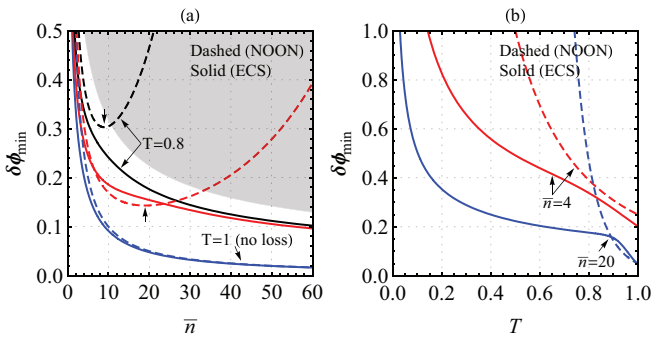

FIG. 1. (Color online) The ultimate precision $\delta\phi_{\min}$ against (a) the number of photons $\bar{n}$ or N and (b) the transmission rate T for the NOON (dashed lines) and the ECS (solid lines) states. In (a), $T = 1$ [blue (dark gray) lines], 0.9 [red (light gray) lines], and 0.8 (black lines). Two arrows indicate $N_{\rm opt} = -2/\ln T$ with $T = 0.8$ and 0.9. In (b), $\bar{n} = 4$ [red (light gray) lines] and 20 [blue (dark gray) lines]. A crossover of $\delta\phi_{\min}$ between the ECS and the NOON states occurs for $\bar{n}$ (or N) $= 20$ and $T \in (0.85, 1)$. The shaded area in (a) is a region where the sensitivity is worse than the shot-noise limit $1/\sqrt{\bar{n}}$.

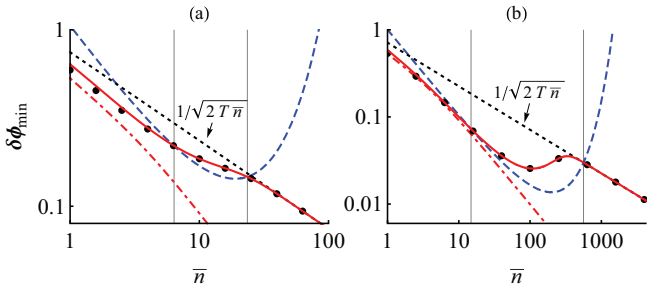

FIG. 2. (Color online) Log-log plot of $\delta\phi_{\min}$ for (a) $T = 0.9$ and (b) $T = 0.99$. Black dotted lines: the classical limit $1/\sqrt{2T\bar{n}}$; blue dashed lines: $\delta\phi_{\min}$ of the NOON state; red solid lines (solid circles): approximated (exact) $\delta\phi_{\min}$ of the ECS; red dot-dashed lines: $\delta\phi_{\min}$ of the ECS in the absence of photon losses (i.e., $T = 1$), given by Eq. (3). The two vertical lines at $\bar{n} = 6.4$ and 23.5 in (a) and $\bar{n} = 14.8$ and 561 in (b) show the crossover of $\delta\phi_{\min}$ between the ECS and the NOON states.

From Fig. 1, we have observed the crossover of $\delta\phi_{\min}$ between the ECS and the NOON states, which can be understood by simply comparing the QFIs for the two states. Without the photon losses, the ultimate precision of the ECS always surpasses those of the NOON states because $F_Q = F_Q^{\rm cl} + F_Q^{\rm HL} > F_{Q,\rm NOON}$ (as $F_Q^{\rm HL} = F_{Q,\rm NOON} = \bar{n}^2$). In the presence of moderate photon losses, the Heisenberg term $F_Q^{\rm HL} \approx (\bar{n}T)^2 e^{-2R\bar{n}}$ decays more quickly than that of the NOON state $F_{Q,\rm NOON} \approx \bar{n}^2 e^{-R\bar{n}}$. This makes it possible for the NOON state to outperform the ECS when the quantum contribution $F_Q^{\rm HL}$ dominates the classical contribution $F_Q^{\rm cl}$. From Fig. 2, one can find that the NOON states with $\bar{n} \in (6.4, 23.5)$ for $R = 0.1$ and $\bar{n} \in (14.8, 561)$ for $R = 0.01$ are preferable, within the vertical lines of Fig. 2.

In general, the crossover condition can be obtained by equating Eqs. (13) and (12). This gives a transcendental equation: $\bar{n}T^{\bar{n}-1} \approx 2 + \bar{n}Te^{-2R\bar{n}}$, whose solution is illuminated by the red solid curve in Fig. 3. It shows that the NOON states outperform the ECS inside the crossover region, while the ECS prevails outside. The upper and the lower boundaries of the region are well fitted by $\bar{n}_u \approx 3.2T^6/R^{1.15}$ (the black dashed line) and $\bar{n}_l \approx 1.4T^{-3}/R^{1/2}$ (the blue dash-dotted line), respectively. The upper boundary corresponds to $F_{Q,\rm NOON} \approx F_Q^{\rm cl}$. As shown in Fig. 3, we find that the crossover of $\delta\phi_{\min}$ between the ECS and the NOON states takes place for $T \in (0.854, 1)$. For such a relatively low loss rate ($0 < R < 0.15$), the precision of the NOON state could surpass that of the ECS over a wider range of $\bar{n}$ until the classical term $F_Q^{\rm cl}$ begins to dominate. Actually, the NOON states with $\bar{n} > \bar{n}_u$ cease to be optimal, and their precision becomes even worse than the classical limit [36]. From Fig. 3, we also note that no crossover occurs for $T \lesssim 0.854$ and the ultimate precision of the ECS is always better than that of the NOON state [see also the black lines in Fig. 1(a)].

IV. DISCUSSIONS AND CONCLUSION

Before closing, we discuss how to prepare the ECS and how to saturate the ultimate phase sensitivity in real experiment. As suggested in Ref. [43], the input ECS can be generated

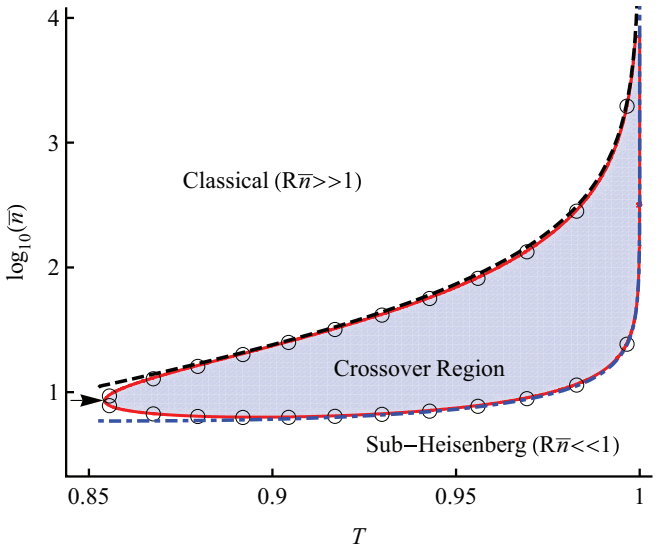

FIG. 3. (Color online) The crossover region in which $\delta\phi_{\min}$ of the NOON state is preferable. Red solid line: $\bar{n}T^{\bar{n}-1} = 2 + \bar{n}Te^{-2R\bar{n}}$ for $R = 1 - T$ and $T \in (0.85,1)$; black dashed and blue dot-dashed lines: $\bar{n}_u \simeq 3.2T^6/R^{1.15}$ and $\bar{n}_l \simeq 1.4T^{-3}/R^{0.5}$, respectively, fitting very well with the boundary of the crossover region (open circles). The critical point of the crossover is $(T,\bar{n}) = (0.854, 8.58)$, as indicated by the arrow.

by passing a coherent state $|\alpha/\sqrt{2}\rangle_1$ and a coherent state superposition $\sim|\alpha/\sqrt{2}\rangle_2 + |-\alpha/\sqrt{2}\rangle_2$ (experimentally available for $\alpha \approx 1.5$ [48]) through the first 50:50 beam splitter. To achieve the ultimate phase sensitivity, we consider the parity measurement with respect to the output state $\hat{\rho}_{\rm out}(\phi) = \hat{B}_{1,2}\hat{\rho}(\phi)\hat{B}_{1,2}^{\dagger}$ [14,17,34,43], where $\hat{B}_{1,2}$ is the second 50:50 beam splitter transformation and $\hat{\rho}(\phi)$ is given by Eq. (7). The output signal can be solved analytically as

$$\langle\hat{\Pi}\rangle = {\rm Tr}[\hat{\rho}_{\rm out}\hat{\Pi}] = 2\mathcal{N}_\alpha^2\left[e^{-T|\alpha|^2} + e^{-|\alpha|^2(1-T\sin\phi)}\cos\left(T|\alpha|^2\cos\phi\right)\right], \quad (15)$$

where $\hat{\Pi} = (-1)^{\hat{a}_1^{\dagger}\hat{a}_1}$ is the parity operator. Due to $\langle\hat{\Pi}^2\rangle = 1$, we have the phase sensitivity $\delta\phi_\Pi = \sqrt{1-\langle\hat{\Pi}\rangle^2}/|\partial\langle\hat{\Pi}\rangle/\partial\phi|$, which in general depends on the value of phase shift ϕ. Without particle loss, i.e., $T = 1$ and $R = 0$, the sensitivity reaches the minimum value $\delta\phi_{\Pi,\,\min} = 1/\sqrt{\bar{n}[\bar{n}+1+w(\bar{n}e^{-\bar{n}})]}$ (almost saturating the quantum Cramér-Rao bound) when the phase shift is equal to its optimal value $\phi_{\min} = \pi/2$. Surprisingly, in the presence of photon loss with arbitrary loss rate, $\delta\phi_\Pi$ diverges at $\phi = \pi/2$ due to the slope of the signal $\partial\langle\hat{\Pi}\rangle/\partial\phi \propto \cos(\phi - T|\alpha|^2\cos\phi) = 0$. The best sensitivity $\delta\phi_{\Pi,\,\min}$ can be obtained for $\phi_{\min}$ symmetrically shifting from $\pi/2$. The lower bound is almost saturated by $\delta\phi_{\Pi,\,\min}$ as long as the photon loss rate $R \lesssim 0.01$. For a larger loss rate, the parity detection cannot saturate the quantum Cramér-Rao bound, and the optimal measurement scheme remains unclear.

In summary, by considering a superposition of NOON states as the "input" of a lossless optical interferometer, we have shown that the quantum Fisher information $F_Q \geqslant \bar{n}^2$ and therefore the ultimate precision of the phase sensitivity can be better than the Heisenberg limit. As a special case of the superposed state, an entangled coherent state $\propto|\alpha,0\rangle_{1,2} + |0,\alpha\rangle_{1,2}$ has been investigated. The exact result of the quantum Fisher information is obtained to investigate the role of photon losses on the lower bound of phase sensitivity $\delta\phi_{\min}$. Without the photon losses, i.e., the absorption rate $R = 0$ and the transmission rate $T = 1$, we confirm that the input ECS always outperforms the NOON state [43]. In the presence of photon losses, the transition of $\delta\phi_{\min}$ from the Heisenberg scaling to the classical limit occurs due to the loss-induced quantum decoherence between the sensor states. The quantum-classical transition depends upon the number of photons being lost $R\bar{n}$, rather than the total photon number $\bar{n}$ or the loss rate R alone. For a given transmission rate $T \in (0.85,1)$, we also find that there exists a crossover of $\delta\phi_{\min}$ between the ECS and the NOON states. The NOON state is preferable in the crossover region, i.e., $\bar{n}T^{\bar{n}-1} \gtrsim 2 + \bar{n}Te^{-2R\bar{n}}$. For $R\bar{n} \gg 1$, however, the precision of the NOON state degrades below the classical limit, while for the ECS state, $\delta\phi_{\min}$ obeys the classical limit $1/\sqrt{2T\bar{n}}$, better than that of the NOON state. The ultimate sensitivity of the input ECS can be reached by parity measurement for a small photon loss rate (e.g., $R \lesssim 0.01$).

Note added. Recently, we notice that the authors in Ref. [49] studied relevant work about the quantum Fisher information of an entangled coherent state with and without photon losses.

ACKNOWLEDGMENTS

We thank Professor D. L. Zhou and Professor J. P. Dowling for helpful discussions. This work is supported by Natural Science Foundation of China (NSFC; Contracts No. 11174028 and No. 11274036), the Fundamental Research Funds for the Central Universities (Contract No. 2011JBZ013), and the Program for New Century Excellent Talents in University (Contract No. NCET-11-0564). X.W.L is partially supported by the National Innovation Experiment Program for University Students.

APPENDIX A: EIGENVALUES AND EIGENVECTORS OF THE REDUCED DENSITY MATRIX

We present a general method to diagonalize a reduced density matrix like Eq. (4). The eigenvector of $\hat{\rho}$ can be spanned as $|\lambda(\phi)\rangle = \sum_j c_j|\Phi_j\rangle$, where the states $|\Phi_j\rangle$ are not necessarily orthogonal. Using the eigenvalue equation $\hat{\rho}|\lambda(\phi)\rangle = \lambda|\lambda(\phi)\rangle$, or, equivalently, $\sum_j\langle\Phi_i|\hat{\rho}|\Phi_j\rangle c_j = \lambda\sum_j\langle\Phi_i|\Phi_j\rangle c_j$, we can determine the eigenvalue λ and the amplitudes c_j. It is convenient to write down the eigenvalue equation in a matrix form: $\boldsymbol{\rho}\mathbf{c} = \lambda\mathbf{A}\mathbf{c}$, where the elements of $\boldsymbol{\rho}$ and $\mathbf{A}$ are $\rho_{ij} = \langle\Phi_i|\hat{\rho}|\Phi_j\rangle$ and $A_{ij} = \langle\Phi_i|\Phi_j\rangle$ and $\mathbf{c} = (c_1,c_2,\ldots)^T$. Multiplying the inverse matrix $\mathbf{A}^{-1}$ on the left, we can rewrite the eigenvalue equation as

$$\tilde{\boldsymbol{\rho}}\mathbf{c} \equiv \mathbf{A}^{-1}\boldsymbol{\rho}\mathbf{c} = \lambda\mathbf{c}, \quad (A1)$$

where $\tilde{\boldsymbol{\rho}} = \mathbf{A}^{-1}\boldsymbol{\rho}$.

Using the above formula, we now diagonalize the reduced density operator of Eq. (4). First, we expand the eigenvectors as $|\lambda(\phi)\rangle = c_1|\Phi_1\rangle + c_2|\Phi_2\rangle$, where $|\Phi_1\rangle = |\sqrt{T}\alpha\rangle_1 = |\sqrt{T}\alpha\rangle_1|0\rangle_2$ and $|\Phi_2\rangle = |\sqrt{T}\alpha e^{i\phi}\rangle_2 = |0\rangle_1|\sqrt{T}\alpha e^{i\phi}\rangle_2$. It is

easy to obtain the matrix

$$\tilde{\boldsymbol{\rho}} = \mathcal{N}_\alpha^2 \begin{pmatrix} 1+e^{-|\alpha|^2} & e^{-T|\alpha|^2}+e^{-R|\alpha|^2} \\ e^{-T|\alpha|^2}+e^{-R|\alpha|^2} & 1+e^{-|\alpha|^2} \end{pmatrix},$$

where T ($R = 1-T$) is the transmission (absorption) rate of the photons and $\mathcal{N}_\alpha^2 = 1/[2(1+e^{-|\alpha|^2})]$. Next, from the equation $|\lambda\mathbf{I} - \tilde{\boldsymbol{\rho}}| = 0$, we obtain the eigenvalues

$$\lambda_\pm = \mathcal{N}_\alpha^2 \left[\left(1+e^{-|\alpha|^2}\right) \pm \left(e^{-T|\alpha|^2}+e^{-R|\alpha|^2}\right) \right], \quad \text{(A2)}$$

which obey $\lambda_- + \lambda_+ = 1$. Substituting $\lambda_\pm$ into Eq. (A1), or $(\lambda\mathbf{I} - \tilde{\boldsymbol{\rho}})\mathbf{c} = 0$, we further obtain the amplitudes $c_1 = \pm c_2$, i.e., the eigenvectors $|\lambda_\pm(\phi)\rangle \propto (\pm|\sqrt{T}\alpha\rangle_1 + |\sqrt{T}\alpha e^{i\phi}\rangle_2)$, as in Eq. (8).

APPENDIX B: DERIVATIONS OF THE QUANTUM FISHER INFORMATION

First, we derive the general expression of the QFI [i.e., Eq. (6)]. For a mixed state $\hat{\rho} = \sum_m \lambda_m |\lambda_m\rangle\langle\lambda_m|$, the QFI is given by the well-known formula of Eq. (5), where the eigenvectors of the reduced density matrix $\{|\lambda_m\rangle\}$ span an othonormalized and complete basis. In general, the dimension of the entire Hilbert space is huge. However, there exists a much smaller subset $\{|\lambda_i\rangle\}$ with nonzero weights λ_i. It is convenient to express the QFI in terms of this subset only. For this purpose, we divide the complete basis $\{|\lambda_m\rangle\}$ into two subsets: $\{|\lambda_i\rangle\}$ and $\{|\lambda_{\bar{i}}\rangle\}$, with $\lambda_i \neq 0$ and $\lambda_{\bar{i}} = 0$, respectively. Using the completeness relation $\sum_{\bar{i}} |\lambda_{\bar{i}}\rangle\langle\lambda_{\bar{i}}| = 1 - \sum_i |\lambda_i\rangle\langle\lambda_i|$, Eq. (5) can be rewritten as

$$F_Q = \sum_i \frac{2\langle\lambda_i|(\hat{\rho}')^2|\lambda_i\rangle}{\lambda_i} + \sum_j \frac{2\langle\lambda_j|(\hat{\rho}')^2|\lambda_j\rangle}{\lambda_j} + \sum_{i,j} 2\left(\frac{1}{\lambda_i+\lambda_j} - \frac{1}{\lambda_i} - \frac{1}{\lambda_j}\right) \left|\langle\lambda_i|\,\hat{\rho}'|\lambda_j\rangle\right|^2, \quad \text{(B1)}$$

where only the subset $\{|\lambda_i\rangle\}$ with $\lambda_i \neq 0$ is involved. Since $\{|\lambda_i\rangle\}$ are orthonormalized, i.e., $\langle\lambda_i|\lambda_j\rangle = \delta_{i,j}$, we have $\langle\lambda_i|\lambda_j'\rangle + \langle\lambda_i'|\lambda_j\rangle = 0$, and hence

$$\langle\lambda_i|(\hat{\rho}')^2|\lambda_i\rangle = (\lambda_i')^2 + \lambda_i^2\langle\lambda_i'|\lambda_i'\rangle + \sum_l (\lambda_l^2 - 2\lambda_i\lambda_l)|\langle\lambda_i'|\lambda_l\rangle|^2,$$

$$|\langle\lambda_i|\hat{\rho}'|\lambda_j\rangle|^2 = (\lambda_i')^2\delta_{i,j} + (\lambda_i - \lambda_j)^2|\langle\lambda_i'|\lambda_j\rangle|^2.$$

Substituting them into Eq. (B1) and using $|\langle\lambda_j'|\lambda_i\rangle|^2 = |\langle\lambda_i'|\lambda_j\rangle|^2$, we obtain the general formula of the QFI as in Eq. (6).

Now, we apply the general formula to calculate the QFI of the ECS state. Since the eigenvalues of the reduced density matrix $\lambda_\pm$ are phase independent, the first term of Eq. (6) vanishes. From Eq. (8), it is easy to obtain the derivation of the eigenvectors,

$$|\lambda_\pm'\rangle = \eta_\pm \frac{\partial}{\partial\phi}|\sqrt{T}\alpha e^{i\phi}\rangle_2 = \eta_\pm \sum_{n=0}^{\infty} in\, d_n(\alpha\sqrt{T}e^{i\phi})\,|n\rangle_2\,, \quad \text{(B2)}$$

where the normalization factors $\eta_\pm = 1/\sqrt{2(1\pm e^{-T|\alpha|^2})}$ and the probability amplitudes of the coherent state $d_n(\alpha) \equiv \langle n|\alpha\rangle = \alpha^n e^{-\frac{1}{2}|\alpha|^2}/\sqrt{n!}$, which satisfy $\sum_n |d_n(\alpha)|^2 = 1$ and

$$\sum_{n=0}^{+\infty} n\,|d_n(\alpha)|^2 = |\alpha|^2, \quad \sum_{n=0}^{+\infty} n^2\,|d_n(\alpha)|^2 = |\alpha|^2(1+|\alpha|^2).$$

Therefore, combining Eqs. (8) and (B2), we obtain

$$\langle\lambda_\pm|\lambda_\pm'\rangle = \eta_\pm^2 \sum_{n=0}^{\infty} in \left|d_n(\alpha e^{i\phi}\sqrt{T})\right|^2 = i\eta_\pm^2|\alpha|^2T \quad \text{(B3)}$$

and, similarly, $\langle\lambda_\mp|\lambda_\pm'\rangle = i\eta_+\eta_-|\alpha|^2T$, as well as $\langle\lambda_\pm'|\lambda_\pm'\rangle = \eta_\pm^2|\alpha|^2T(1+|\alpha|^2T)$. These results enable us to calculate the remaining terms of Eq. (6):

$$\sum_{i=\pm}\lambda_i F_{Q,i} = 4\lambda_+\eta_+^2|\alpha|^2T(1+|\alpha|^2T - \eta_+^2|\alpha|^2T) + 4\lambda_-\eta_-^2|\alpha|^2T(1+|\alpha|^2T - \eta_-^2|\alpha|^2T) \quad \text{(B4)}$$

and

$$\sum_{i=\pm,j=\mp} \frac{8\lambda_i\lambda_j}{\lambda_i+\lambda_j}\left|\langle\lambda_i'|\,\lambda_j\rangle\right|^2 = 16\lambda_+\lambda_-\eta_+^2\eta_-^2|\alpha|^4T^2 \quad \text{(B5)}$$

due to $\lambda_+ + \lambda_- = 1$. Finally, we get the exact result of the QFI for the input ECS:

$$F_Q = 4\mathcal{N}_\alpha^2|\alpha|^2T \times \left[1+|\alpha|^2T - \mathcal{N}_\alpha^2|\alpha|^2T\left(1+\frac{1-e^{-2R|\alpha|^2}}{1-e^{-2T|\alpha|^2}}\right)\right],$$

where we have used the relations $\lambda_+\eta_+^2 + \lambda_-\eta_-^2 = \mathcal{N}_\alpha^2$ and $4\lambda_+\lambda_-\eta_+^2\eta_-^2 = \mathcal{N}_\alpha^4[1-e^{-2R|\alpha|^2}]$, as well as

$$\lambda_+\eta_+^4 + \lambda_-\eta_-^4 = \frac{\mathcal{N}_\alpha^2}{2}\frac{1-e^{-|\alpha|^2}}{1-e^{-2T|\alpha|^2}}.$$

Using $\bar{n} = 2\mathcal{N}_\alpha^2|\alpha|^2$ and hence $|\alpha|^2 = \bar{n} + w(\bar{n}e^{-\bar{n}})$, the QFI can be further simplified as Eq. (9).

[1] C. M. Caves, Phys. Rev. D **23**, 1693 (1981).
[2] B. Yurke, S. L. McCall, and J. R. Klauder, Phys. Rev. A **33**, 4033 (1986).
[3] M. J. Holland and K. Burnett, Phys. Rev. Lett. **71**, 1355 (1993).
[4] D. J. Wineland, J. J. Bollinger, W. M. Itano, and D. J. Heinzen, Phys. Rev. A **50**, 67 (1994).
[5] D. Leibfried, M. D. Barrett, T. Schaetz, J. Britton, J. Chiaverini, W. M. Itano, J. D. Jost, C. Langer, and D. J. Wineland, Science **304**, 1476 (2004).
[6] M. W. Mitchell, J. S. Lundeen, and A. M. Steinberg, Nature (London) **429**, 161 (2004).
[7] V. Giovannetti, S. Lloyd, and L. Maccone, Nat. Photonics **5**, 222 (2011); Science **306**, 1330 (2004).

[8] A. Luis, Phys. Lett. A **329**, 8 (2004).
[9] A. M. Rey, L. Jiang, and M. D. Lukin, Phys. Rev. A **76**, 053617 (2007).
[10] S. Boixo, A. Datta, S. T. Flammia, A. Shaji, E. Bagan, and C. M. Caves, Phys. Rev. A **77**, 012317 (2008).
[11] S. Choi and B. Sundaram, Phys. Rev. A **77**, 053613 (2008).
[12] M. J. Woolley, G. J. Milburn, and C. M. Caves, New J. Phys. **10**, 125018 (2008).
[13] Y. C. Liu, G. R. Jin, and L. You, Phys. Rev. A **82**, 045601 (2010); G. R. Jin, Y. C. Liu, and L. You, Front. Phys. **6**, 251 (2011).
[14] J. J. Bollinger, W. M. Itano, D. J. Wineland, and D. J. Heinzen, Phys. Rev. A **54**, R4649 (1996).
[15] T. Kim, O. Pfister, M. J. Holland, J. Noh, and J. L. Hall, Phys. Rev. A **57**, 4004 (1998).
[16] R. A. Campos, C. C. Gerry, and A. Benmoussa, Phys. Rev. A **68**, 023810 (2003).
[17] J. P. Dowling, Contemp. Phys. **49**, 125 (2008); P. M. Anisimov, G. M. Raterman, A. Chiruvelli, W. N. Plick, S. D. Huver, H. Lee, and J. P. Dowling, Phys. Rev. Lett. **104**, 103602 (2010).
[18] B. Lücke, M. Scherer, J. Kruse, L. Pezzé, F. Deuretzbacher, P. Hyllus, O. Topic, J. Peise, W. Ertmer, J. Arlt, L. Santos, A. Smerzi, and C. Klempt, Science **334**, 773 (2011).
[19] C. W. Helstrom, *Quantum Detection and Estimation Theory* (Academic, New York, 1976).
[20] A. S. Holevo, *Probabilistic and Statistical Aspects of Quantum Theory* (North-Holland, Amsterdam, 1982).
[21] S. L. Braunstein and C. M. Caves, Phys. Rev. Lett. **72**, 3439 (1994).
[22] S. L. Braunstein, C. M. Caves, and G. J. Milburn, Ann. Phys. (N.Y.) **247**, 135 (1996).
[23] S. Luo, Phys. Rev. Lett. **91**, 180403 (2003).
[24] L. Pezzé and A. Smerzi, Phys. Rev. Lett. **102**, 100401 (2009).
[25] M. Kacprowicz, R. Demkowicz-Dobrzański, W. Wasilewski, K. Banaszek, and I. A. Walmsley, Nat. Photonics **4**, 357 (2010).
[26] Z. Sun, J. Ma, X. M. Lu, and X. Wang, Phys. Rev. A **82**, 022306 (2010).
[27] J. Ma, Y. X. Huang, X. Wang, and C. P. Sun, Phys. Rev. A **84**, 022302 (2011).
[28] M. G. Genoni, S. Olivares, and M. G. A. Paris, Phys. Rev. Lett. **106**, 153603 (2011); M. G. Genoni, S. Olivares, D. Brivio, S. Cialdi, D. Cipriani, A. Santamato, S. Vezzoli, and M. G. A. Paris, Phys. Rev. A **85**, 043817 (2012).
[29] B. M. Escher, L. Davidovich, N. Zagury, and R. L. de Matos Filho, Phys. Rev. Lett. **109**, 190404 (2012).
[30] W. Zhong, Z. Sun, J. Ma, X. Wang, and F. Nori, Phys. Rev. A **87**, 022337 (2013).
[31] M. D. Lang and C. M. Caves, arXiv:1306.2677.
[32] A. N. Boto, P. Kok, D. S. Abrams, S. L. Braunstein, C. P. Williams, and J. P. Dowling, Phys. Rev. Lett. **85**, 2733 (2000).
[33] C. C. Gerry, Phys. Rev. A **61**, 043811 (2000).
[34] C. C. Gerry, A. Benmoussa, and R. A. Campos, Phys. Rev. A **66**, 013804 (2002).
[35] H. Lee, P. Kok, and J. P. Dowling, J. Mod. Opt. **49**, 2325 (2002).
[36] U. Dorner, R. Demkowicz-Dobrzański, B. J. Smith, J. S. Lundeen, W. Wasilewski, K. Banaszek, and I. A. Walmsley, Phys. Rev. Lett. **102**, 040403 (2009); R. Demkowicz-Dobrzański, U. Dorner, B. J. Smith, J. S. Lundeen, W. Wasilewski, K. Banaszek, and I. A. Walmsley, Phys. Rev. A **80**, 013825 (2009).
[37] B. M. Escher, R. L. de Matos Filho, and L. Davidovich, Nat. Phys. **7**, 406 (2011); Braz. J. Phys. **41**, 229 (2011).
[38] R. Demkowicz-Dobrzański, J. Kolodynski, and M. Guta, Nat. Commun. **3**, 1063 (2012).
[39] S. J. van Enk, Phys. Rev. A **72**, 022308 (2005).
[40] T.-W. Lee, S. D. Huver, H. Lee, L. Kaplan, S. B. McCracken, C. J. Min, D. B. Uskov, C. F. Wildfeuer, G. Veronis, and J. P. Dowling, Phys. Rev. A **80**, 063803 (2009).
[41] J. J. Cooper, D. W. Hallwood, and J. A. Dunningham, Phys. Rev. A **81**, 043624 (2010).
[42] S. Knysh, V. N. Smelyanskiy, and G. A. Durkin, Phys. Rev. A **83**, 021804(R) (2011).
[43] J. Joo, W. J. Munro, and T. P. Spiller, Phys. Rev. Lett. **107**, 083601 (2011); J. Joo, K. Park, H. Jeong, W. J. Munro, K. Nemoto, and T. P. Spiller, Phys. Rev. A **86**, 043828 (2012).
[44] M. Jarzyna and R. Demkowicz-Dobrzański, Phys. Rev. A **85**, 011801(R) (2012).
[45] J. J. Cooper, D. W. Hallwood, J. A. Dunningham, and J. Brand, Phys. Rev. Lett. **108**, 130402 (2012).
[46] C. C. Gerry and P. L. Knight, *Introductory Quantum Optics* (Cambridge University Press, Cambridge, 2005).
[47] T. Ono and H. F. Hofmann, Phys. Rev. A **81**, 033819 (2010); H. F. Hofmann, *ibid.* **79**, 033822 (2009); H. F. Hofmann and T. Ono, *ibid.* **76**, 031806(R) (2007); A. Luis, *ibid.* **64**, 054102 (2001).
[48] A. Ourjoumtsev, R. Tualle-Brouri, J. Laurat, and P. Grangier, Science **312**, 83 (2006); A. Ourjoumtsev, H. Jeong, R. Tualle-Brouri, and P. Grangier, Nature (London) **448**, 784 (2007); H. Takahashi, K. Wakui, S. Suzuki, M. Takeoka, K. Hayasaka, A. Furusawa, and M. Sasaki, Phys. Rev. Lett. **101**, 233605 (2008); T. Gerrits, S. Glancy, T. S. Clement, B. Calkins, A. E. Lita, A. J. Miller, A. L. Migdall, S. W. Nam, R. P. Mirin, and E. Knill, Phys. Rev. A **82**, 031802(R) (2010).
[49] X. Jing, J. Liu, W. Zhong, and X. Wang, arXiv:1307.8009; J. Liu, X. Jing, and X. Wang, Phys. Rev. A **88**, 042316 (2013).